Science of the Total Environment 647 (2019) 29–36

Contents lists available at ScienceDirect

Science of the Total Environment

journal homepage: www.elsevier.com/locate/scitotenv

Urbanization and climate change: Insights from eco-hydrological diagnostics

Danlu Cai [a,*], Klaus Fraedrich [b], Yanning Guan [a,*], Shan Guo [a], Chunyan Zhang [a], Xiuhua Zhu [c]

[a] Institute of Remote Sensing and Digital Earth, Chinese Academy of Sciences, Beijing, China
[b] Max-Planck-Institute for Meteorology, Hamburg, Germany
[c] KlimaCampus, Hamburg University, Hamburg, Germany

HIGHLIGHTS

- Nighttime lighted urbanization is subjected to eco-hydrological analysis.
- Urbanization shows differences between developing and developed countries.
- Bi-modal and uni-modal distributions characterize Chinese and US-American cities.
- Chinese cities follow climate induced 'wet-gets-drier' and 'dry-gets-wetter' changes.
- Global urbanization develops towards uni-modality.

GRAPHICAL ABSTRACT

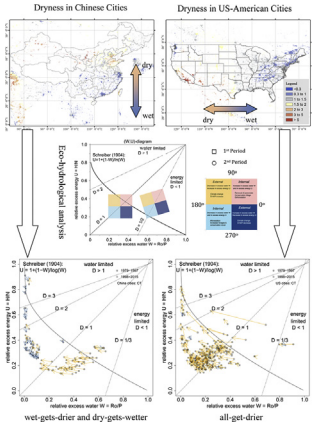

ARTICLE INFO

Article history:
Received 24 October 2017
Received in revised form 16 July 2018
Accepted 23 July 2018
Available online 23 July 2018

Editor: R Ludwig

Keywords:
Urban climate
Rainfall-runoff chain
Climate and anthropogenic induced changes
Developing and developed countries

ABSTRACT

To quantify how urbanization induced long-term changes have altered the evolution of urban climate, a novel eco-hydrological diagnostic is introduced and applied globally, to a developing and a developed country (China and US-America). Urban areas are (i) geographically identified by remote sensing based nighttime light, (ii) physically embedded in state spaces spanned by suitable combinations of surface energy and water fluxes comprising the rainfall-runoff chain, and (iii) dynamically characterized by the time evolution of the surface fluxes at geographically fixed locations, analyzed as trajectories in state space, and interpreted by an attribution model separating anthropogenic from climate induced causes. The results describe the long term climatological settings of urban areas in a net radiation versus dryness diagram, while the attribution of change is diagnosed in a state space spanned by energy and water excess: (i) Cities in China are characterized by a bi-modal distribution separated by the boundary between water and energy-limited (northern and southern) regimes while US-American cities are assembling unimodally on this boundary, and globally the urbanized areas are also aligned along this boundary between water and energy-limited regimes. (ii) Attribution of eco-hydrological changes of urbanized regions to climate and human-induced causes shows also basic differences between the developing and developed country: urbanization in Chinese cities is characterized by a 'wet-gets-drier' and 'dry-gets-wetter' paradigm of the climate-induced contributions, due to which cities tend towards a unimodal state as it is observed for US-American urban areas. Finally, implications for large scale city planning are discussed in the outlook.

© 2018 Elsevier B.V. All rights reserved.

* Corresponding authors.
E-mail addresses: caidl@radi.ac.cn (D. Cai), guanyn@radi.ac.cn (Y. Guan).

https://doi.org/10.1016/j.scitotenv.2018.07.319
0048-9697/© 2018 Elsevier B.V. All rights reserved.

1. Introduction

Although global and regional climate changes are known to have an impact on altering the urban surface climate, urbanization is one of the most evident aspects of human modification of natural landscapes and climate (Cai et al., 2017; Fan et al., 2017). Urbanization, which can be interpreted as anthropogenic induced change in surface fluxes, includes the effects of increasing atmospheric greenhouse gas concentration, aerosol emission, and land use and land cover change, is a major driver for the formation and evolution of urban climates (Grimm et al., 2008; Wu and Yang, 2013). Numerous observational studies have reported that cities experience urban heat island effect and pollutant emissions a decade ahead of the global average (Briber et al., 2013; Carreiro et al., 2009; Dentener et al., 2006; Friedlingstein et al., 2006; George et al., 2007; Zhou et al., 2017). These long-term changes may have altered the ecology or evolution of urban organisms in ways that can occur outside the cities in the future (Carreiro and Tripler, 2005; Youngsteadt et al., 2017).

Current approaches are limited in analyzing effects of urbanization/anthropogenic induced surface driven parameter changes (e.g. temperature, carbon and nitrogen) on response variables (e.g. biomass and water) over ecologically relevant spatial and temporal scales (Youngsteadt et al., 2017). Experiments are inevitably constrained by the number of driver variables to be tested simultaneously (Leuzinger et al., 2011). And, as the number of change drivers increases, understanding the interacting mechanisms causing a particular net response becomes much more difficult (Larsen et al., 2011). Contrarily, quantitative analyses of rainfall–runoff chain dynamics on watershed scales as part of the climate system will physically relate water demand to supply by combining the energy and water flux balances (Cai et al., 2016; Cai et al., 2015).

The rainfall–runoff chain dynamics is subjected to an analysis based on the Budyko framework (Budyko, 1974), which has inspired physical insights on the control of the water and energy balance, employing a functional relationship between water demand by net radiation (or potential evapotranspiration) and water supply by precipitation. It reduces the complex mutual interactions between climate and hydrological processes to a single parameter, the dryness as the ratio of two fluxes: mean annual net radiation versus precipitation (Donohue et al., 2009; Fraedrich and Sielmann, 2011; Potter et al., 2005; Williams et al., 2012, for a theoretical analysis, see Fraedrich (2010)). In addition, the coupled water–energy budget and the separation of its respective variables into water and energy related flux ratios provide an eco-hydrological diagnostics that can attribute total change to impacts of external or climate and internal or land-use/watershed change (Tomer and Schilling, 2009; Wang and Hejazi, 2011; Zhan et al., 2014).

Thus, embedding urbanization processes into the changing rainfall–runoff chain with the aim to quantify how urbanization induced long-term changes have altered the evolution of urban climate for a developing and a developed country (China and US-America), has to our knowledge not been performed. In a broader sense, this study expands on the quantitative analyses of urbanization. Commencing with basic measures characterizing the thermal climate effected by urbanization (Cai et al., 2017), a more comprehensive metric is now being employed to embed urbanization into its eco-hydrological environment. In this sense (as a big image) urbanization analysis emerges as a three-step scheme conditional on geographical and economical structures, which are based on night-light clustering and on the separation between developed and developing countries (US-America and China): First, urbanization (as human habitat) is embedded in the thermally effected climate (Cai et al., 2017). This is followed by an eco-hydrological urbanization analysis to attribute causes of change to climate and/or human induced forcing employing causality models based on the Budyko framework. As an outlook, the subsequent next focus will turn towards biodiversity as it can be measured by species and endangered species.

That is, after describing urbanization and the thermal environment of Chinese and US-American cities, we now analyze urbanization and climate change to gain insights from an eco-hydrological diagnostics employing the Budyko framework. Although varying subsurface storage in the catchment water balance is neglected, it provides a simple subgrid closure relation that quantifies how spatial heterogeneity affects average annual evapotranspiration at catchment scales (see Freund and Kirchner, 2017). It is this scale-sensitive aspect which requires special attention. Urbanization and effects on the living world will be considered in the further work.

Thus, after identifying urban areas by remote sensing based nighttime light, urban areas are physically embedded in state spaces spanned by the coupled eco-hydrological conceptual models (Section 2) comprising the rainfall-runoff chain. The dynamical time evolutions of the surface energy and water fluxes of China and America are analyzed as trajectories in state space, and interpreted by separating anthropogenic from climate induced causes (Section 3) before a concluding summary (Section 4).

2. Data and methods of analysis

The geographical setting of urban regions is described by nighttime light signals derived from the Defense Meteorological Satellite Program's Operational Line Scan System (DMSP/OLS). The nighttime light data provides striking remotely sensed information as the basis to analyze global spatiotemporal changes of urbanization processes (Elvidge et al., 1997; Small and Elvidge, 2011; Small et al., 2005; Sutton, 2003). Spatially contiguous lighted pixels obtained from global nighttime stable light products 2012 with digital value number $DN \geq 12$ are defined as cities. The DN-threshold reduces the effects of over-glow usually caused by anthropogenic activities in undeveloped areas, which is excluded from the urban development statistics (Elvidge et al., 1997; Small et al., 2005). Urbanization dynamics are analyzed within the Budyko framework (Fig. 1a–b) to describe hydro-ecological setting and evaluate the changes. They are based on the balanced land surface fluxes net radiation, precipitation and runoff averaged over the following two almost twenty year periods (1979 to 97 and 98 to 2015) ERA-Interim of ECMWF (Balsamo et al., 2012). For detailed calculations, see Cai et al. (2017) and for descriptions of data quality control and threshold selection, see Small et al. (2011).

2.1. Budyko's diagram of climate forcing

The rainfall–runoff chain receives a total supply of water and energy which, interpreted as forcing fluxes, are balanced by a flux partitioning. That is, rainfall P is balanced by runoff Ro and evapotranspiration E, and net radiation N or potential evapotranspiration, which, representing atmospheric water demand, is balanced by the sensible heat flux H and evapotranspiration E:

$$P = Ro + E \text{ and } N = H + E \tag{1}$$

The forcing flux ratio of energy-over water supply, that is of net radiation N over rainfall P, has been introduced by Budyko (1974) as dryness $D = N / P$. It separates energy-limited regimes ($D < 1$ or $N < P$) from water-limited ones ($D > 1$, $N > P$) at $D = 1$. Note that, for compatibility, energy fluxes are given in terms of water equivalents (m/year).

Budyko's geobotanic climate (N,D)-diagram is a surface climate state space spanned by net radiation versus dryness (Fig. 1a). It represents the climatological forcing and, in a qualitative and idealized sense, the meridionality (from polar to equatorial latitudes) and zonality (from wetter western to drier eastern parts in the mid-latitudes) of continental climates. Moreover, climate variables can be displayed, such as precipitation, presented by the slopes of lines through the origin, $N = D$ P, or the total supply, $N = (P + N)[D / (D + 1)]$, as isolines which attain the slope $N + P$ at the origin ($N = D = 0$). Finally, the dryness index or

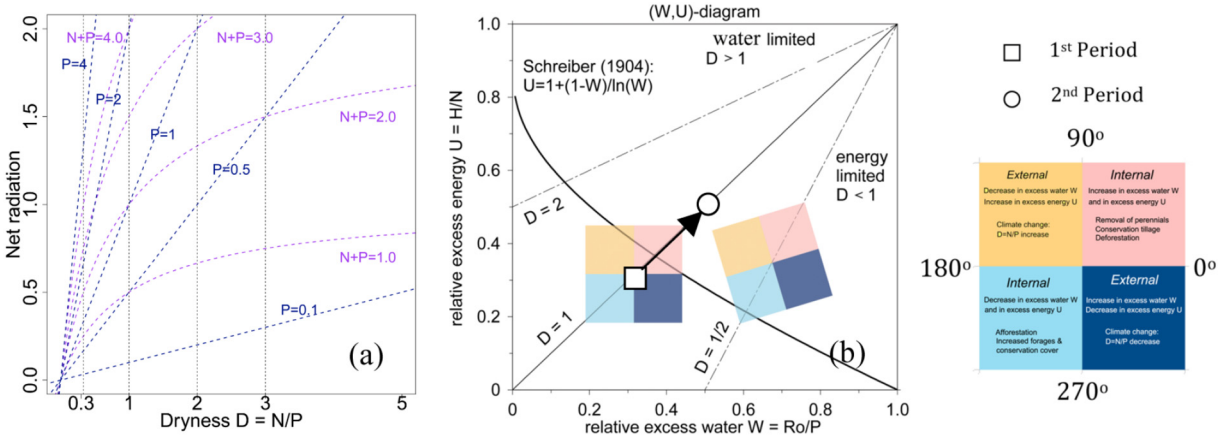

Fig. 1. Climate and ecohydrological state space: (a) (N, D)-diagram spanned by the mean net radiation N and dryness ratio D (all units in m/year water equivalent). Precipitation $N = PD$ corresponds to the slope of straight lines through the origin; the curve of total supply of energy and water satisfies $N = (N + P)[D / (D + 1)]$, and (b) (U,W)-diagram spanned by relative excess water W (runoff versus precipitation) and energy U (sensible heat flux versus net radiation) with lines of constant dryness D (net radiation versus precipitation). The rainfall–runoff chain related to Budyko's framework can also be included in the ecohydrological state space: $U = 1 + (1 - W) / \log(W)$ represented by the empirical formula from Schreiber (1904) (for the stochastic interpretation as an ideal rainfall–runoff chain, see Fraedrich, 2010). (For interpretation of the references to color in this figure, the reader is referred to the web version of this article.)

the moisture available for plant growth is best expressed in terms of the seasonal course of soil water content (Prentice et al., 1992). It enables a classification of geobotanical climate states, it has also been used to include the biosphere into a physical-based framework of climate analysis (detailed description see Budyko (1974) and Cai et al. (2014)).

2.2. Eco-hydrological diagram: flux dynamics and partitioning

Characterizing the eco-hydrological environment requires a separation of energy and water fluxes to display ratios of the partitioning fluxes to balance the respective forcing which, to our knowledge has been suggested first by Milne et al. (2002). That is, the relative excess energy U as the portion of energy supply not being used for evapotranspiration and the relative excess water W, as the portion of water supply not being used by the ecosystem and thus available for geomorphological formation. Usually both flux ratios are bounded within the interval (0,1), represented by the water and energy limits of the rainfall–runoff chain. Fig. 1b displays the (U,W) plane showing the lines of constant dryness, $U = 1 + (W - 1) / D$, through the $(U = 1, W = 1)$ point, whose slopes represent (inverse) aridity ratios:

$$U = H/N = 1 - E/N \text{ and } W = Ro/P = 1 - E/P \quad (2)$$

with $D = N / P = (1 - W) / (1 - U)$. Note that the (U,W)-axes through their respective origin at $W = 1 - E / P = 0$ and at $U = 1 - E / N = 0$ define natural limits of the energy and water flux dynamics; they are characterized by $N = E$ and $P = E$, respectively, as upper limits of evapotranspiration not to exceed the energy-water supply (note that oasis effects are excluded).

This state space is introduced here (i) to amend Budyko's diagram of the rainfall-runoff chain's forcing by the eco-hydrologically balanced flux partitioning associated with the forcing, and (ii) to estimate the causalities of change by the following attribution analysis. This analysis is based on an eco-hydrological ansatz, which provides a diagnostic model of trajectories in (U,W)-space due to changes of the external (or climate) forcing and/or of the internal (or anthropogenic) partitioning; the diagnostic model depends on the regional dryness state attained by the system at the origin of the trajectory of change (for a detailed description see Cai et al., 2016).

(i) *Changes caused by internal processes - flux partitioning of rainfall-runoff-chain*: Assume constant climate forcing (P and N constant) but evapotranspiration having changed over time; then, $dU = -dE / N$ and $dW = -dE / P$ represent an internal change in flux partitioning (say dE) affecting the watershed, such as a change in vegetation or land surface, which results in a deviation towards the positive diagonal (Fig. 1b, first (pink) quadrant and third (light blue) quadrant).

(ii) *Changes caused by external processes - forcing of rainfall-runoff chain*: Assume that E is constant, then $dD > 0$ ($dD < 0$) leads to increasing (or decreasing) $U = 1 - E / N$ and decreasing (or increasing) $W = 1 - E / P$. That is, climate-induced change occurs along the negative diagonal directed towards the second (yellow) quadrant and fourth (dark blue) quadrant (see Fig. 1b).

2.3. Spatial-temporal heterogeneity and Budyko framework

Note that the grid resolution in nighttime light or reanalysis data is typically translated directly onto the Earth's surface, which is recorded as temporal layers at spatial scales of kilometers or degrees. At this scale, much of the variability in the surface climatology of the landscape and its consequences for land–atmosphere interactions may be lost. The potential importance of this aggregation problem has motivated research into methods for capturing sub-grid-scale properties and processes within Earth system models (Beven, 1995; Freund and Kirchner, 2017). Numerous modeling studies have shown that averaged surface schemes tend to overestimate evapotranspiration and sensible heat flux (e.g., Ershadi et al., 2013; Essery et al., 2003; Giorgi and Avissar, 1997; Klink, 1995) and this overestimation bias is largest where topographic effects play a major role (Pope and Stratton, 2002; Boyle and Klein, 2010; Bacmeister et al., 2014).

Budyko showed empirically that under steady-state conditions in catchments without significant groundwater inputs, losses, or storage changes, the long-term annual average evapotranspiration (ET) rate is functionally related to both the supply of moisture from the atmosphere (precipitation, P) and net irradiance (available energy) as an estimator of the evaporative demand for water by the atmosphere (potential evapotranspiration, PET). Freund and Kirchner (2017) use Budyko curves to derive a simple sub-grid closure relation that quantifies how spatial heterogeneity affects average ET as seen from the atmosphere. Our analysis focuses on analyzing urbanization dynamics in two long-term periods, based on long-term averaged grid scale atmospheric forcing trajectories within the Budyko's framework in two different non-dimensional sets of axes. Thus, by considering changes, the possible

overestimation bias from the grid resolution may be assumed to be negligible.

3. Applying climate and eco-hydrological state space diagnostics to urbanization in China, US-America and on the globe

Urbanization or urban ecosystem change is the consequence of both climate change and local anthropogenic activities. First, the equilibrium surface climate state is comprised as a frequency distribution in the climate or (N,D)-state space of net radiation and dryness representing meridionality (N) and zonality (D) of the urban surface climate in the Budyko's framework (Section 3.1). We employ eco-hydrological analysis methods (Renner and Bernhofer, 2012; Tomer and Schilling, 2009) to diagnose the controlling factors of the rainfall–runoff chain on urban scale, to analyze the forces underlying the changes of the long-term average fluxes coupling soil, vegetation, hydrologic and atmospheric compartments, and to attribute their causes (Section 3.2). For analysis two almost twenty-year intervals (1979 to 97 and 1998 to 2015) have been selected, which represent the climates characterized by a trend and a hiatus (almost no-trend) period (Vuille et al., 2015). Employing the Budyko framework prevents the results to depend on simple scaling, because the state space coordinates are non-dimensional flux ratios. However, multiple scaling processes characterizing, for example, long term memory (LTM) and the recurrence of extremes, may affect the underlying equilibrium and the assumption of stationarity, but only if these processes contain periods with large amplitudes exceeding the fifteen to twenty-year time interval chosen for analysis. Re-analyses and direct observational data of state variables characterizing the energy and water balance, have been subjected to LTM analyses (see for example, Fig. 2 in Fraedrich and Blender 2003, and Fig. 3 in Wang et al., 2010) have revealed the following results: After detrending, the near surface temperatures over land show long term memory or scaling to be absent over the continents except for the transitional coastal areas while soil moisture scaling is regionally changing with weak to vanishing memory in the highly urbanized areas of China and US-America. Therefore, although multiscale or anomalous scaling cannot be excluded in ecohydrological time series, we do not consider their effect for the aim of our analysis of changes on decadal and longer time scales focusing on the highly urbanized locations. It should be noted that city boundaries or human habitation regions are indicated from the satellite-derived observations of spatially contiguous stable anthropogenic light in 2012 (see Section 2) as the study regions.

3.1. Distributions in climate state space

The physical states of global land and cities in the (N,D) diagram are characterized by the number density of area units of (N,D) pairs, whose long-term means (1979–2015) are obtained from the ERA-Interim dataset (Fig. 2a–b): (i) The boundaries include all *973*, *165* and *90* urban pixels associated with (N,D)-pairs on the Global, US-America and China urban land surface, respectively. The zero frequency boundary (or contour line) of global land (Fig. 2a) is comparable with the boundary of the geobotanic zonality (biome) distribution in Budyko (1974) and Cai et al. (2014) (see Fig. 2b–c in Cai et al. (2014)). (ii) Frequency distributions of both global land and city-only in the (N,D)-diagram are characterized by two modes which are separated by meridional differentiation (net radiation ~ 1 m/year), while the distribution of dryness is unimodal with its maximum close to the separation between energy and water limited regimes ($D \sim 1$). (iii) Finally, it should be noted that global cities are statistically more concentrated towards net radiation $N \sim 1$ m/year and $D \sim 1$, amongst 88% (12%) are in the Northern (Southern) Hemisphere. It is also important to note that in the global economic system, ~90% of the world's population lives in the Northern Hemisphere (Jacobs, n.d.).

Geographically, mainland China shares a similar meridional band with the mainland US-America in the Northern Hemisphere (about 20°–55°N vs. 25°–50°N), and zonally, the most densely urbanized/populated parts of China and US-America are in their east. Rings of decreasing urbanization/population density radiate out from the major urban centers of Beijing, Shanghai, and Guangzhou (New York, Philadelphia, and Washington) in China and US. The dryness ratio D, however, increases from south-to-north in China versus east-to-west in US, which is due to the influence of the Tibetan Plateau. Chinese population geographer Hu (1935) draws a "geo-demographic demarcation line" from Heihe (northeast) to Tengchong (southwest) separating a western (eastern) area cover 64% (36%) occupied by a population of 4% (96%). Despite an epic urban migration, until 2015, the western (eastern) parts of China comprise 57% (43%) of the area but only 6% (94%) of the population. In contrast, the western US-America remains lightly populated except for several large cities and with a dense population in Southern California.

Climatologically, China and US-America can be embedded into a physical state space spanned by water and energy flux to provide insights in differentiating urban ecosystems in developing and developed countries (China and US-America), the physical states of China and US-America cities in the (N,D)-diagram (Fig. 2c–d) characterizing a climatological meridionality: (i) Mainland China and US-America cities share similar net radiation or latitude ranges in the Northern Hemisphere. The dryness ratio D, however, for Chinese cities spreads over a dryness domain of $0.3 < D < 3$, while US-America cities cluster along $D \sim 1$. Cities in the dry regions of the western US-America are less visible in the (N, D) diagram of ERA-Interim scale, even for the densest populations in Southern California. (ii) Frequency distribution of Chinese cities in the (N,D)-diagram is characterized by two modes separated by dryness differentiation ($D \sim 1$), while frequency distribution of US-America cities is unimodal with its maximum close to the separation of energy- and water limited regimes ($D \sim 1$). The two modes of Chinese cities can be related to climates of northern and southern China.

3.2. Attribution of change in eco-hydrological state space

The ecohydrological Ansatz originally suggested by Tomer and Schilling (2009) adheres to the assumption that internal/anthropogenic (or external/climate) changes are independent of the regional state of aridity at the origin of the trajectory of change. However, this assumption may be an issue if applied to regional-scale change where the original aridity state differs from the fixed baseline (aridity index $D = 1$). The method used follows Cai et al. (2016) incorporating the aridity of the initial state into the eco-hydrological attribution ecohydrological attribution model and upgrade the equation accounting for the aridity index using the assumption of orthogonality between climatic and anthropogenic changes to quantify the impacts on evapotranspiration/runoff and predict land-cover changes in line with vegetation damage diagnostics.

For a better understanding of how urban climate systems have responded to urbanization, eco-hydrological change analysis in the (U,W)-plane is employed. It captures the change of long-term averaged states which satisfy the water and energy balance of the coupled soil, vegetation, hydromorphologic, and atmospheric compartments (Milne et al., 2002). States shifting from one (long term) averaging period to the next are traced (Fig. 1b; see also Fig. 2 in Tomer and Schilling (2009)) as pieces of trajectories that, due to coordinates separating water and energy supplies, provide a direct measure of the causes of change induced by external (climate) forcing and internal (anthropogenic) processes in both a developing and a developed country (China and US-America). The following results are noted:

(i) Change vectors (arrows) represent pieces of trajectories which indicate eco-hydrological shifts between a first and a second period, whose coordinate system (or the four quadrants of attribution) depends on initial dryness ratio ranging from 0° to 360°.

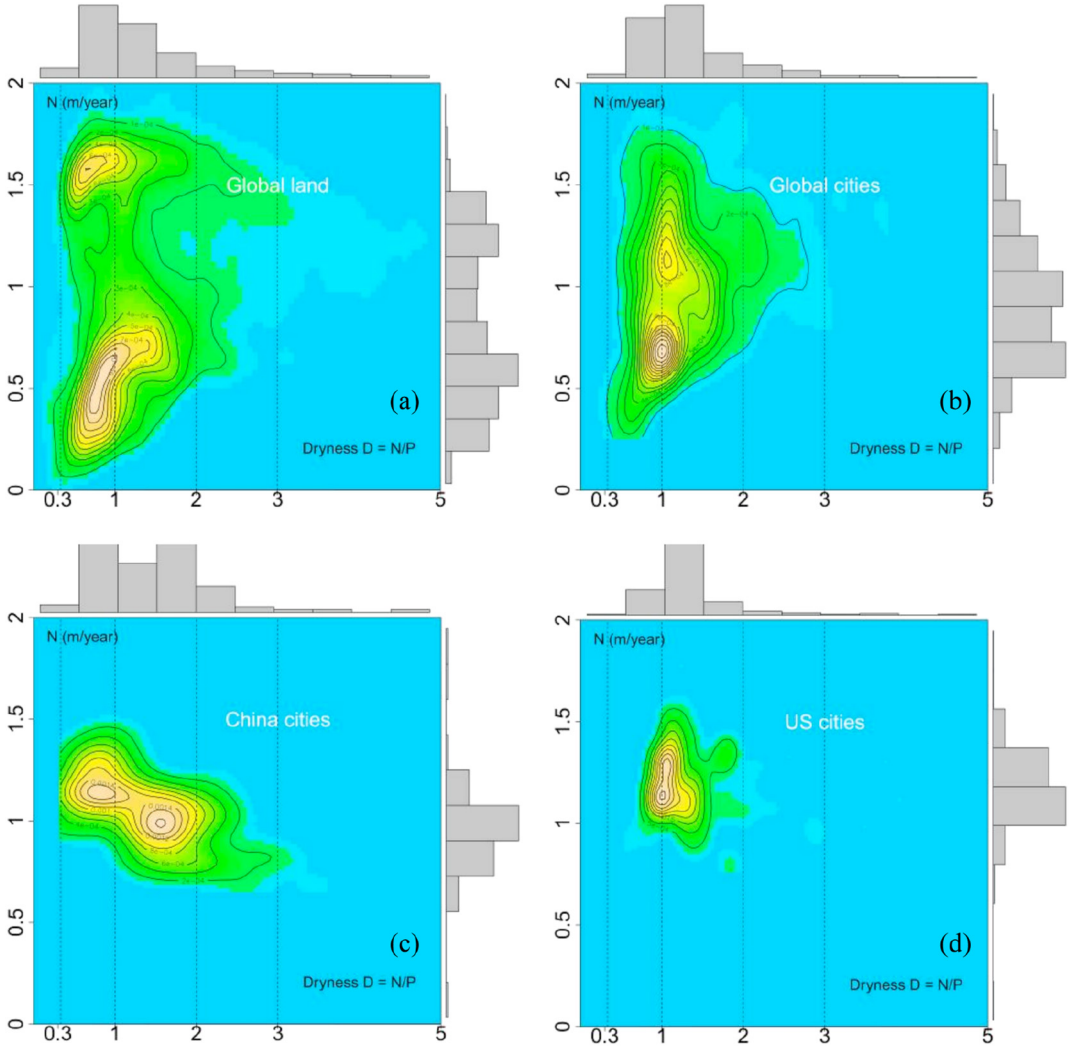

Fig. 2. Frequency distribution of the climatological means of net radiation and dryness or (N,D) pairs (from ERA-Interim): (a) global land, (b) global cities, (c) China cities and (d) US-American cities. The total land area corresponds to the total number of equal area units. The $D = 1$ threshold separating energy-limited from water-limited regimes (vertical line) is included.

(ii) Attribution (Fig. 3a–b) in China (US) shows external or climate (second or fourth quadrant, yellow or dark blue) and internal or anthropogenic (first or third quadrant, pink or light blue) induced changes that affect 32.43% or 29.22% and 14.80% or 23.55% (87.85% or 4.37% and 2.00% or 5.78%) of the respective areas; that is, changes are predominantly caused by external processes in 61.65% in China (92.22% in US). Attribution (Fig. 3c–d) in China (US) cities shows external (second or fourth quadrant, orange or dark blue) and internal (first or third quadrant, pink or light blue) induced changes that affect 40.00% or 25.2% and 2.1% or 32.6% (88.8% or 3.6% and 3.6% or 4.1%) of the respective areas. In summarizing, even in city regions, external climate induced forces dominate the eco-hydrological change observed in China and US-America cities (65.26% vs. 92.31%).

(iii) Time evolution is represented by a flow in the eco-hydrological (U,W)-space showing pieces of trajectories where the climate CT and anthropogenic induced AT processes are separated. Compared to a developing country like China, these cities appear not to be dominated by an urban sprawl linked to an expanding area (Fig. 3c). External changes in US-American cities are governed by a pronounced 'all-gets-drier' (Fig. 3d) mechanism controlled by climate induced forcing mostly clustering in the domain of the distribution monopoly near a $D \sim 1$ city-equilibrium, see also (Feng and Fu, 2013; Sherwood and Fu, 2014).

The four quadrants attribution in Fig. 3 shows that external change dominates Chinese urbanization in last two decades, although the land used for urban construction in China has expanded in all directions from the original core function zone, while no obvious urban area expanding pattern in the main city zone of America could be found (see Fig. 1c–e and Table 1 in Cai et al. (2017)). The details of urban change attribution differences to investigate and quantify urban climate changes on subcontinental scale and distinguish developing and developed countries (China and US-America) are revealed in Fig. 4:

Climate induced change in China is governed by flows emerging from the initially dry (wet) city modes of northern (southern) China along the water limit $W \sim 0$ (near the energy limit of $U \sim 0.2$). That is, the evolution of the initially separated two urban modes (Fig. 2c), which are related to northern and southern Chinese cities, is characterized by the paradigm of a systematic 'dry-gets-wetter' and 'wet-gets-drier' trend, respectively, finally converging towards the $D = 1$ threshold bound near $U > 0.2$. As non-city regimes in China do not reveal a preferential (climate induced) direction of the trajectories (not shown) an urbanization-climate coupling mechanism appears to account for this finding. It is plausible that also the internal changes (Fig. 4c, d) show a common tendency towards the origin (U,W) ≥ 0. This impervious urbanization effect demonstrated in eco-hydrological state space bears some similarity to the situation of terminal lakes in a dry basin, with cities being run with runoff not leaving their watershed.

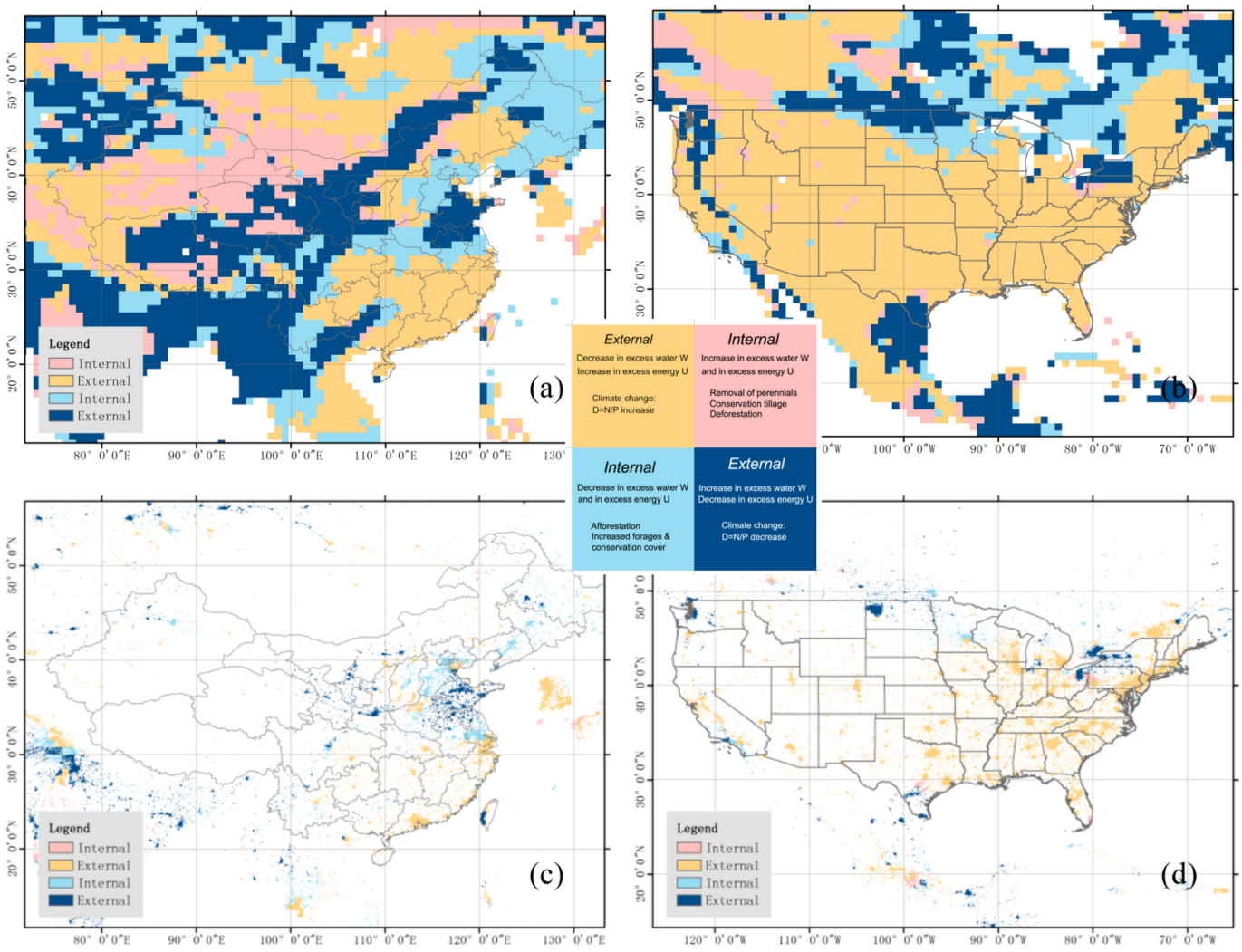

Fig. 3. Distributions of attribution classes of ecohydrological change separating internal from external causes. Geographical distributions of the four quadrants of attribution depending on initial dryness ratio in (a–b) China and US, and (c–d) in the related spatially contiguous lighted areas with DN ≥ 12 are classified as cities (detailed descriptions of data quality control and threshold selection see Small et al. (2011)). (For interpretation of the references to color in this figure, the reader is referred to the web version of this article.)

In summarizing, city or human habitation regions are determined from the satellite-derived high space resolution observations of spatially contiguous stable anthropogenic light in 2012 as the study regions. Employing the Budyko framework provides a quantitative description of the long-term average rainfall-runoff chain, which is characterized by balanced annual water and energy fluxes at catchment scales neglecting changes in subsurface storage in the catchment. In this sense the attribution analysis presented here is quasi-stationary and fluctuations within steady state are not considered. The Budyko framework is recently used to assess the hydrological conditions beyond the steady state assumption in closed terrestrial water balances (Arora, 2002; Greve et al., 2015). Esquivel-Hernández et al. (2017) use the Budyko (1974) and Tomer–Schilling (2009) frameworks to analyze the hydroclimatic conditions and their influence on the ecohydrological resistance and resilience across six different biomes of Costa Rica between 1989 and 2005. These may be meaningful and relevant and should, therefore, be taken into account in future work, because resilience may provide a useful metric to characterize urbanization in combination with the effects of climate and human induced forcing.

4. Conclusions

The globally increasing urbanization process, where human population, material demands of production, human consumption and urban waste discharge expand and become more intense (Alberti, 2005; Johnson, 2001; Montgomery, 2008; Pataki et al., 2006), has recently emerged as a major component for the formation and evolution of urban climates (Grimm et al., 2008; Wu and Yang, 2013). It affects not only the climates on local and regional scale, but also the water resources, air quality, human health, biodiversity and ecosystem functioning (Platt et al., 1994).

Besides studying individual megacities, research on global/countrywide urbanization requires the definition of urban boundary, which can be different depending on the questions being addressed (Schneider and Woodcock, 2008, see also http://blogs.worldbank.org/sustainablecities/what-does-urban-mean). The traditional socio-demographic definitions considering administrative boundaries, population size or density, and economic indicators (Utzinger and Keiser, 2006) may be fundamentally flawed, because human settlement patterns and, more generally, land surface modification can be represented as continuous spatial variation in intensity of development or degree of modification (Small et al., 2011). Thus, the remote sensing based technique of physical human-made nighttime light of continuous areas is used in this study to define a land use based geographical state of urbanization, which is a relatively recent field of research. It has potential to obtain more comprehensive characteristics relating to urban dynamics and associated environmental consequences during the urbanization processes (Cai et al., 2017; Ma et al., 2012).

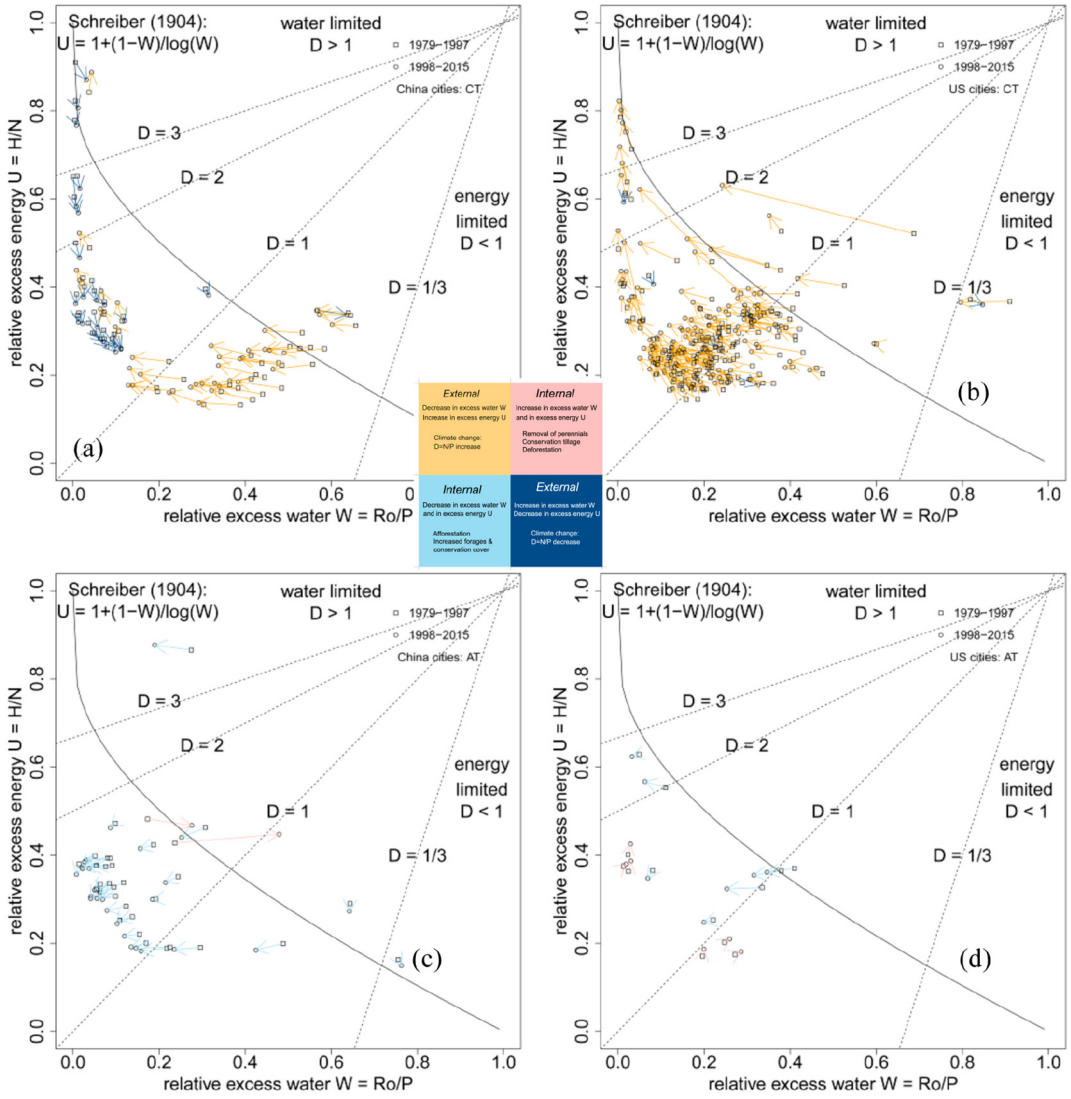

Fig. 4. Ecohydrological states are denoted by squares and circles: The reference states (squares) represent the first period, which is followed by subsequent shift to the second period (circles). Directions and lengths of arrows connecting first with second period provide the attribution of change of the internal/anthropogenic (external/climate) partitioning (see text): (a–b) external partitioning in China and US cities; and (c–d) internal partitioning in China and US cities.

There are numerous studies focusing on the impact of urbanization on the surface driver parameter changes (e.g. temperature, CO_2 and N, see Table 1 in Wu and Yang (2013)) and thus to the response variables (e.g. biomass and water) over ecologically relevant spatial and temporal scales (Youngsteadt et al., 2017). However, considerable inconsistencies inevitably exist in the increasing number of driver variables tested simultaneously (Leuzinger et al., 2011). On the other hand, understanding the interacting mechanisms causing a particular net response becomes much more difficult with an increasing the number of drivers of change (Larsen et al., 2011). Therefore, this study physically relates water demand to supply combining energy and water flux balances as part of the climate system to investigate and quantify urban climate changes on global and subcontinental scale and distinguishing developing and developed countries (China and US-America). Main conclusions are as follows:

(i) The zero frequency boundary (or contour line) which comprises all urban areas is comparable with that of global land which, in the (N, D) diagram reveals climate states of two statistical modes separated in meridionality (by the water demand or net radiation of about $N \sim 1$ m/year), while the distribution is unimodal with respect to dryness with the maximum close to the separation of energy from water limited regimes ($D \sim 1$). Note that global cities are more concentrated towards net radiation $N \sim 1$ m/year and $D \sim 1$.

(ii) Cities in China are characterized by a bi-modal distribution in the (N, D) diagram which are related to the northern and southern Chinese cities. The two urban modes in China are separated by the boundary separating water from energy limited regimes ($D \sim 1$) while US-American cities are assembling unimodally on this boundary as well as global urbanized areas.

(iii) Long-term urbanization processes have altered the evolution of urban climate, which are noticed by separating the climate and anthropogenic induced pieces of trajectories in the eco-hydrological space. Compared to the 'almost all-get-drier' paradigm governing the US-American cities, the evolution of the initially separated two urban modes in China is governed by the paradigm of a systematic 'dry-gets-wetter' and 'wet-gets-drier' trend which are finally converging finally converging towards the $D = 1$ threshold as US-American/global cities.

In last two decades, the land used for urban construction in China has expanded in all directions from the original core function zone. Here we observe that the eco-hydrological states move systematically

towards the energy and water limits, $E = N$ and $E = P$, indicating augmentation of the water cycle driven by changing vegetation, climate and human interactions. The impervious urbanization effect demonstrated in eco-hydrological state space bears some similarity to the situation of terminal lakes in a dry basin, with cities being run with runoff not going outside of their watershed.

Acknowledgments

Support by the National Science Foundation of China (Grant 41501375), by Key Laboratory of Satellite Mapping Technology and Application, National Administration of Surveying, Mapping, and Geoinformation (Grant KLSMTA-201710), and by the Max Planck Fellow Group (DC, KF) is acknowledged. We also appreciate a reviewer's suggestion to discuss scale differences between observables and the theoretical model in more detail.

References

Alberti, M., 2005. The effects of urban patterns on ecosystem function. Int. Reg. Sci. Rev. 28, 168–192.
Arora, V.K., 2002. The use of the aridity index to assess climate change effect on annual runoff. J. Hydrol. 265, 164–177.
Bacmeister, J.T., et al., 2014. Exploratory high-resolution climate simulations using the Community Atmosphere Model (CAM). J. Clim. 27, 3073–3099.
Balsamo, G., et al., 2012. A global land-surface reanalysis based on ERA-Interim meteorological forcing. ERA-Report Series (25 pp.).
Beven, K., 1995. Linking parameters across scales: subgrid parameterizations and scale dependent hydrological models. Hydrol. Process. 9, 507–525.
Boyle, J., Klein, S.A., 2010. Impact of horizontal resolution on climate model forecasts of tropical precipitation and diabatic heating for the TWP-ICE period. J. Geophys. Res. Atmos. 115. https://doi.org/10.1029/2010JD014262.
Briber, B.M., Hutyra, L.R., Dunn, A.L., Raciti, S.M., Munger, J.W., 2013. Variations in atmospheric CO2 mixing ratios across a Boston, MA urban to rural gradient. Land 2, 304–327.
Budyko, M., 1974. Climate and Life. vol. 18. Academic Press (508 pp.).
Cai, D., Fraedrich, K., Sielmann, F., Guan, Y., Guo, S., Zhang, L., Zhu, X., 2014. Climate and vegetation: an ERA-Interim and GIMMS NDVI Analysis. J. Clim. 27, 5111–5118.
Cai, D., Fraedrich, K., Sielmann, F., Zhang, L., Zhu, X., Guo, S., Guan, Y., 2015. Vegetation dynamics on the Tibetan Plateau (1982 to 2006): an attribution by eco-hydrological diagnostics. J. Clim. 28, 4576–4584.
Cai, D., Fraedrich, K., Sielmann, F., Guan, Y., Guo, S., 2016. Land-cover characterization and aridity changes of South America (1982–2006): an attribution by ecohydrological diagnostics. J. Clim. 29, 8175–8189.
Cai, D., Fraedrich, K., Guan, Y., Guo, S., Zhang, C., 2017. Urbanization and the thermal environment of Chinese and US-American cities. Sci. Total Environ. 589, 200–211.
Carreiro, M.M., Tripler, C.E., 2005. Forest remnants along urban-rural gradients: examining their potential for global change research. Ecosystems 8, 568–582.
Carreiro, M.M., Pouyat, R.V., Tripler, C.E., Zhu, W.-X., 2009. Carbon and nitrogen cycling in soils of remnant forests along urban–rural gradients: case studies in the New York metropolitan area and Louisville, Kentucky. Ecology of Cities and Towns: A Comparative Approach. Cambridge University Press, New York, pp. 308–328.
Dentener, F., et al., 2006. Nitrogen and sulfur deposition on regional and global scales: a multimodel evaluation. Glob. Biogeochem. Cycles 20. https://doi.org/10.1029/2005GB002672.
Donohue, R.J., McVICAR, T., Roderick, M.L., 2009. Climate-related trends in Australian vegetation cover as inferred from satellite observations, 1981–2006. Glob. Chang. Biol. 15, 1025–1039.
Elvidge, C.D., Baugh, K.E., Kihn, E.A., Kroehl, H.W., Davis, E.R., 1997. Mapping city lights with nighttime data from the DMSP Operational Linescan System. Photogramm. Eng. Remote. Sens. 63, 727–734.
Ershadi, A., McCabe, M., Evans, J.P., Walker, J.P., 2013. Effects of spatial aggregation on the multi-scale estimation of evapotranspiration. Remote Sens. Environ. 131, 51–62.
Esquivel-Hernández, G., Sánchez-Murillo, R., Birkel, C., Good, S.P., Boll, J., 2017. Hydroclimatic and ecohydrological resistance/resilience conditions across tropical biomes of Costa Rica. Ecohydrology 10. https://doi.org/10.1002/eco.1860.
Essery, R., Best, M., Betts, R., Cox, P.M., Taylor, C.M., 2003. Explicit representation of subgrid heterogeneity in a GCM land surface scheme. J. Hydrometeorol. 4, 530–543.
Fan, C., et al., 2017. Understanding the impact of urbanization on surface urban heat islands-a longitudinal analysis of the oasis effect in subtropical desert cities. Remote Sens. 9. https://doi.org/10.3390/rs9070672.
Feng, S., Fu, Q., 2013. Expansion of global drylands under a warming climate. Atmos. Chem. Phys. 13, 10,081–10,094.
Fraedrich, K., 2010. A parsimonious stochastic water reservoir: Schreiber's 1904 equation. J. Hydrometeorol. 11, 575–578.
Fraedrich, K., Blender, R., 2003. Scaling of atmosphere and ocean temperature correlations in observations and climate models. Phys. Rev. Lett. 90, 108501 (1-4).
Fraedrich, K., Sielmann, F., 2011. An equation of state for land surface climates. Int. J. Bifurcation Chaos 21, 3577–3587.
Freund, E.R., Kirchner, J.W., 2017. A Budyko framework for estimating how spatial heterogeneity and lateral moisture redistribution affect average evapotranspiration rates as seen from the atmosphere. Hydrol. Earth Syst. Sci. 21, 217.
Friedlingstein, P., et al., 2006. Climate–carbon cycle feedback analysis: results from the C4MIP model intercomparison. J. Clim. 19, 3337–3353.
George, K., Ziska, L.H., Bunce, J.A., Quebedeaux, B., 2007. Elevated atmospheric CO2 concentration and temperature across an urban–rural transect. Atmos. Environ. 41, 7654–7665.
Giorgi, F., Avissar, R., 1997. Representation of heterogeneity effects in earth system modeling: experience from land surface modeling. Rev. Geophys. 35, 413–437.
Greve, P., Gudmundsson, L., Orlowsky, B., Seneviratne, S.I., 2015. The Budyko framework beyond stationarity. Hydrol. Earth Syst. Sci. Discuss. 12. https://doi.org/10.5194/hessd-5112-6799-2015.
Grimm, N.B., Faeth, S.H., Golubiewski, N.E., Redman, C.L., Wu, J., Bai, X., Briggs, J.M., 2008. Global change and the ecology of cities. Science 319, 756–760.
Hu, H., 1935. Distribution of China's population: accompanying charts and density map. Acta Geograph. Sin. 2, 33–74.
Jacobs, F., d. Pop by Lat and Pop by Long. Available online at. http://bigthink.com/strange-maps/563-pop-by-lat-and-pop-by-long.
Johnson, M.P., 2001. Environmental impacts of urban sprawl: a survey of the literature and proposed research agenda. Environ. Plan. A 33, 717–735.
Klink, K., 1995. Surface aggregation and subgrid-scale climate. Int. J. Climatol. 15, 1219–1240.
Larsen, K.S., et al., 2011. Reduced N cycling in response to elevated CO2, warming, and drought in a Danish heathland: synthesizing results of the CLIMAITE project after two years of treatments. Glob. Chang. Biol. 17, 1884–1899.
Leuzinger, S., Luo, Y., Beier, C., Dieleman, W., Vicca, S., Körner, C., 2011. Do global change experiments overestimate impacts on terrestrial ecosystems? Trends Ecol. Evol. 26, 236–241.
Ma, T., Zhou, C., Pei, T., Haynie, S., Fan, J., 2012. Quantitative estimation of urbanization dynamics using time series of DMSP/OLS nighttime light data: a comparative case study from China's cities. Remote Sens. Environ. 124, 99–107.
Milne, B.T., Gupta, V.K., Restrepo, C., 2002. A scale invariant coupling of plants, water, energy, and terrain. Ecoscience 9, 191–199.
Montgomery, M.R., 2008. The urban transformation of the developing world. Science 319, 761–764.
Pataki, D., et al., 2006. Urban ecosystems and the North American carbon cycle. Glob. Chang. Biol. 12, 2092–2102.
Platt, R.H., Rowntree, R.A., Muick, P.C., 1994. The Ecological City: Preserving and Restoring Urban Biodiversity. Univ of Massachusetts Press (304 pp.).
Pope, V., Stratton, R., 2002. The processes governing horizontal resolution sensitivity in a climate model. Clim. Dyn. 19, 211–236.
Potter, N., Zhang, L., Milly, P., McMahon, T.A., Jakeman, A., 2005. Effects of rainfall seasonality and soil moisture capacity on mean annual water balance for Australian catchments. Water Resour. Res. 41. https://doi.org/10.1029/2004WR003697.
Prentice, I., Cramer, W., Harrison, S., Leemans, R., Monserud, R., Solomon, A., 1992. A global biome model based on plant physiology and dominance, soil properties and climate. J. Biogeogr. 19, 117–134.
Renner, M., Bernhofer, C., 2012. Applying simple water-energy balance frameworks to predict the climate sensitivity of streamflow over the continental United States. Hydrol. Earth Syst. Sci. 16, 2531–2546.
Schneider, A., Woodcock, C.E., 2008. Compact, dispersed, fragmented, extensive? A comparison of urban growth in twenty-five global cities using remotely sensed data, pattern metrics and census information. Urban Stud. 45, 659–692.
Sherwood, S., Fu, Q., 2014. A drier future. Science 343, 737–739.
Small, C., Elvidge, C.D., 2011. Mapping decadal change in anthropogenic night light. Procedia Environ Sci 7, 353–358.
Small, C., Pozzi, F., Elvidge, C.D., 2005. Spatial analysis of global urban extent from DMSP-OLS night lights. Remote Sens. Environ. 96, 277–291.
Small, C., Elvidge, C.D., Balk, D., Montgomery, M., 2011. Spatial scaling of stable night lights. Remote Sens. Environ. 115, 269–280.
Sutton, P.C., 2003. A scale-adjusted measure of "urban sprawl" using nighttime satellite imagery. Remote Sens. Environ. 86, 353–369.
Tomer, M.D., Schilling, K.E., 2009. A simple approach to distinguish land-use and climate-change effects on watershed hydrology. J. Hydrol. 376, 24–33.
Utzinger, J., Keiser, J., 2006. Urbanization and tropical health—then and now. Ann. Trop. Med. Parasitol. 100, 517–533.
Vuille, M., Franquist, E., Garreaud, R., Casimiro, L., Sven, W., Cáceres, B., 2015. Impact of the global warming hiatus on Andean temperature. J. Geophys. Res. Atmos. 120, 3745–3757.
Wang, D., Hejazi, M., 2011. Quantifying the relative contribution of the climate and direct human impacts on mean annual streamflow in the contiguous United States. Water Resour. Res., 47 https://doi.org/10.1029/2010WR010283.
Wang, G., Dolman, A.J., Blender, R., Fraedrich, K., 2010. Fluctuation regimes of soil moisture in ERA-40 re-reanalysis data. Theor. Appl. Climatol. 99, 1–8. https://doi.org/10.1007/s00704-009-0111-3.
Williams, C.A., et al., 2012. Climate and vegetation controls on the surface water balance: synthesis of evapotranspiration measured across a global network of flux towers. Water Resour. Res., 48 https://doi.org/10.1029/2011WR011586.
Wu, K., Yang, X., 2013. Urbanization and heterogeneous surface warming in eastern China. Chin. Sci. Bull. 58, 1363–1373.
Youngsteadt, E., Ernst, A.F., Dunn, R.R., Frank, S.D., 2017. Responses of arthropod populations to warming depend on latitude: evidence from urban heat islands. Glob. Chang. Biol. 23, 1436–1447.
Zhan, C., Zeng, S., Jiang, S., Wang, H., Ye, W., 2014. An integrated approach for partitioning the effect of climate change and human activities on surface runoff. Water Resour. Manag. 28, 3843–3858.
Zhou, B., Rybski, D., Kropp, J.P., 2017. The role of city size and urban form in the surface urban heat island. Sci. Rep. UK 7. https://doi.org/10.1038/s41598-41017-04242-41592.